Enstrophy Cascade in Decaying Two-Dimensional Quantum Turbulence

Matthew T. Reeves,[1,2,*] Thomas P. Billam,[3,†] Xiaoquan Yu,[1] and Ashton S. Bradley[1]
[1]Department of Physics, Centre for Quantum Science, and Dodd-Walls Centre for Photonic and Quantum Technologies, University of Otago, Dunedin, New Zealand
[2]Australian Research Council Centre of Excellence in Future Low-Energy Electronics Technologies, School of Mathematics and Physics, University of Queensland, St Lucia, QLD 4072, Australia
[3]Joint Quantum Centre (JQC) Durham–Newcastle, School of Mathematics and Statistics, Newcastle University, Newcastle upon Tyne NE1 7RU, United Kingdom
(Received 14 February 2017; published 31 October 2017)

We report evidence for an enstrophy cascade in large-scale point-vortex simulations of decaying two-dimensional quantum turbulence. Devising a method to generate quantum vortex configurations with kinetic energy narrowly localized near a single length scale, the dynamics are found to be well characterized by a superfluid Reynolds number $\mathrm{Re_s}$ that depends only on the number of vortices and the initial kinetic energy scale. Under free evolution the vortices exhibit features of a classical enstrophy cascade, including a k^{-3} power-law kinetic energy spectrum, and constant enstrophy flux associated with inertial transport to small scales. Clear signatures of the cascade emerge for $N \gtrsim 500$ vortices. Simulating up to very large Reynolds numbers ($N = 32\,768$ vortices), additional features of the classical theory are observed: the Kraichnan-Batchelor constant is found to converge to $C' \approx 1.6$, and the width of the k^{-3} range scales as $\mathrm{Re_s}^{1/2}$.

DOI: 10.1103/PhysRevLett.119.184502

Introduction.—Quantum vortices in atomic Bose-Einstein condensates (BECs) offer the possibility not only to physically realize the point-vortex model envisaged by Onsager [1] but also to observe and manipulate it at the level of individual quanta. Experiments have recently demonstrated controllable generation of quantum vortices [2–5], hard-wall trapping potentials containing large, uniform density condensates [6,7], and measurements of vortex circulation [8] and vortex decay processes [2,9,10]. Since well-separated 2D quantum vortices behave as idealized point vortices [11,12], two-dimensional quantum turbulence (2DQT) can be considered a "stripped-down" model of hydrodynamic turbulence with a definite number of degrees of freedom, and thus studying the analogies between 2DQT and 2D classical turbulence (2DCT) may expand our understanding of universal turbulent phenomena. The recent experimental observation of a von Kármán vortex street and the transition to turbulence in the wake of a stirring obstacle [13], for example, adds to evidence that the classical Reynolds number concept may be generalized to turbulence in superfluids [14–16].

The enstrophy cascade of decaying 2DCT predicted by Batchelor [17] is a key process of classical turbulence for which the quantum analogue has remained unexplored. While much theoretical attention has focused on the inverse energy cascade of forced turbulence [18–22] and vortex clustering in negative temperature equilibria [23–26], a clear demonstration of an enstrophy cascade has yet to be presented. A challenge in numerically demonstrating such a cascade in 2DQT is obtaining a sufficiently large vortex number and range of wave numbers k to identify the steep associated energy spectrum $E(k) \propto k^{-3}$ over a significant range of scale space.

In this Letter we directly simulate an N-point-vortex model of decaying 2D quantum turbulence at large N. We devise a method of constructing an initial condition with a large energy contained within a single wave number, allowing us to simulate the 2DQT analog of a scenario where the existence of an enstrophy cascade is well established in 2DCT [27,28]. The system is found to be well-characterized by a superfluid Reynolds number $\mathrm{Re_s}$ that depends only on the number of vortices and the initial wave number k_i. We show that under free evolution the k^{-3} spectrum of the enstrophy cascade emerges for $N \gtrsim 500$, and the associated enstrophy and energy fluxes are found to agree with the Batchelor theory. By increasing N up to 32 768, additional key features of the theory are verified: the Kraichnan-Batchelor constant is found to be $C' \approx 1.6$, close to the accepted classical value, and the length of the inertial range scales as $\mathrm{Re_s}^{1/2}$.

Background.—Turbulent flows at large Reynolds numbers (Re) can spontaneously develop self-similar *cascade* solutions, in which quantities are conservatively transported across a subregion of scale space called the inertial range. Two-dimensional turbulence cannot support the usual Kolmogorov energy cascade of 3D turbulence, since the mean square vorticity, or *enstrophy* is unable to be amplified through vortex stretching. However, Batchelor [17] hypothesized that the enstrophy itself could therefore undergo a cascade, from small to large wave numbers, via a filamentation of vorticity patches. The enstrophy cascade is signified by a kinetic energy spectrum $E(k) = C'\eta^{2/3}k^{-3}$ (subject to a weak logarithmic correction [29]), where η is the enstrophy dissipation rate, assumed equal to the enstrophy flux in the inertial range, and C' is the Kraichnan-Batchelor constant. The lossless cascade terminates at a dissipation

wave number $k_d \sim k_i \mathrm{Re}^{1/2}$, at which viscous dissipation becomes important. The enstrophy cascade must be accompanied by a drift of energy to small wave numbers, in order to be simultaneously consistent with the conservation laws of energy and enstrophy. Importantly, however, strong, long-lived coherent vortices, strongly dependent on the initial conditions, appear and can inhibit the self-similar cascade [28,30,31]. These laminar objects typically introduce a steeper spectral slope [32,33], on top of the k^{-3} turbulent background, recoverable via filtering [34].

Model.—We consider a quantum fluid, such as a BEC, characterized by healing length ξ and speed of sound c, carrying quantized vortices of charge $\kappa_i = \pm 1$ and circulation $\Gamma_i = \kappa_i \Gamma$ [35]. For a quasi-2D system, vortex bending is suppressed and the dynamics become effectively two-dimensional [36]. In the low Mach number limit, where the average intervortex distance ℓ is much greater than the healing length ξ, interactions between vortices and density fluctuations can be ignored on scales $\gtrsim \xi$. In this limit a fully compressible (e.g., Gross-Pitaevskii [37]) description, that complicates interpretation of fluxes [38], is not needed. Instead, the motion of the ith quantum vortex, located at $\mathbf{r}_i$, can be described by a dissipative point-vortex model [39] with compressible effects (at length scales $\lesssim \xi$) added phenomenologically [38,40]. The motion of the ith quantum vortex, located at $\mathbf{r}_i$, is given by

$$\frac{d\mathbf{r}_i}{dt} = \mathbf{v}_i + \mathbf{w}_i; \quad \mathbf{v}_i = \sum_{j=1, j\neq i}^{N} \mathbf{v}_i^{(j)}; \quad \mathbf{w}_i = -\gamma \kappa_i \hat{\mathbf{e}}_3 \times \mathbf{v}_i, \tag{1}$$

where γ is the dissipation rate, $\hat{\mathbf{e}}_3$ is a unit vector perpendicular to the fluid plane, and $\mathbf{v}_i$ and $\mathbf{w}_i$ are the conservative and dissipative parts of the velocity, respectively. The dissipation rate γ arises from thermal friction due to the normal fluid component, here assumed to be stationary [9]. Phenomenologically, we remove opposite-sign vortex pairs separated by less than ξ (modeling dipole annihilation), and smoothly increase the dissipation γ for same-sign vortex pairs as their separation decreases to around ξ (modeling sound radiation by accelerating vortices [41]). Details are provided in the Supplemental Material [42].

The velocity of the ith vortex due to the jth, $\mathbf{v}_i^{(j)}$, is obtained from a Hamiltonian point-vortex model subject to appropriate boundary conditions. We consider a doubly periodic square box [51–54] with side length $L \gg \xi$, for which [55]

$$\mathbf{v}_i^{(j)} = \frac{\pi c \kappa_j}{(L/\xi)} \sum_{m=-\infty}^{\infty} \begin{pmatrix} \frac{-\sin(y'_{ij})}{\cosh(x'_{ij}-2\pi m)-\cos(y'_{ij})} \\ \frac{\sin(x'_{ij})}{\cosh(y'_{ij}-2\pi m)-\cos(x'_{ij})} \end{pmatrix}, \tag{2}$$

where $(x'_{ij}, y'_{ij})/(2\pi/L) \equiv \mathbf{r}_{ij} \equiv \mathbf{r}_i - \mathbf{r}_j$. The absence of a physical boundary offers the usual advantage: vortices cannot reach their own images, enforcing conservation of the (zero) net vorticity. This helps achieve statistical homogeneity and isotropy, as required for comparison with Batchelor's theory.

Spectrum.—The kinetic energy spectrum (per unit mass) in the periodic box is given by [23]

$$E(\mathbf{k}) = E_{\mathrm{self}}(\mathbf{k}) + E_{\mathrm{int}}(\mathbf{k}) \tag{3}$$

$$= \frac{\Gamma^2}{8(\pi k L)^2}\left(N + 2\sum_{i=1}^{N}\sum_{j=i+1}^{N} \langle \kappa_i \kappa_j \cos(\mathbf{k}\cdot\mathbf{r}_{ij})\rangle\right), \tag{4}$$

where $\mathbf{k} = (n_x \Delta k, n_y \Delta k)$ for $n_x, n_y \in \mathbb{Z}$, $\Delta k = 2\pi/L$, and $\langle\cdot\rangle$ denotes ensemble averaging. The average kinetic energy is $\sum_{\mathbf{k}} E(\mathbf{k})(\Delta k)^2 = E_{\mathrm{self}} + E_{\mathrm{int}}$. The self-energy term is, for fixed N, a cutoff-dependent constant, set by L and the vortex core structure at wave numbers $k \gtrsim \xi^{-1}$ [23] (not considered here). The time evolution of $E(\mathbf{k})$ governs the spectral transport of kinetic energy: $dE(\mathbf{k})/dt = T(\mathbf{k}) + D(\mathbf{k})$, where $T(\mathbf{k})$ is the transfer function, given by

$$T(\mathbf{k}) = -\frac{\Gamma^2}{4(\pi k L)^2}\sum_{i=1}^{N}\sum_{j=i+1}^{N} \langle \kappa_i \kappa_j \sin(\mathbf{k}\cdot\mathbf{r}_{ij})\mathbf{k}\cdot(\mathbf{v}_i - \mathbf{v}_j)\rangle, \tag{5}$$

and $D(\mathbf{k})$ is the dissipation spectrum, obtained from Eq. (5) by setting $\mathbf{v} \to \mathbf{w}$. As usual, the enstrophy and energy spectra are related via $\Omega(\mathbf{k}) = 2k^2 E(\mathbf{k})$. Like its classical counterpart, the superfluid transfer function $T(\mathbf{k})$ conservatively redistributes energy, with $\sum_{\mathbf{k}} T(\mathbf{k})(\Delta k)^2 = 0$. The dissipation spectrum $D(\mathbf{k})$ governs the rate of energy loss: $\sum_{\mathbf{k}} D(\mathbf{k})(\Delta k)^2 = dE/dt < 0$. Angularly integrated spectral measures $E(k) = \int d\phi_{\mathbf{k}} k E(\mathbf{k})$, etc., are analyzed by defining a discrete angular integral over a ring of wave numbers: $\tilde{f}(n\Delta k) = \sum_{\mathbf{k}\in\mathcal{D}_n} f(\mathbf{k})\Delta k$, where $\mathcal{D}_n = \{\mathbf{k} | (n-1/2)\Delta k \leq |\mathbf{k}| \leq (n+1/2)\Delta k\}$, and $n = 1, 2, \ldots$. Hence we may define the discrete energy and enstrophy fluxes [56,57]

$$\tilde{\Pi}_\epsilon(n\Delta k) = -\sum_{m=1}^{n} \tilde{T}(m\Delta k)\Delta k, \tag{6}$$

$$\tilde{\Pi}_\omega(n\Delta k) = -2\sum_{m=1}^{n} (m\Delta k)^2 \tilde{T}(m\Delta k)\Delta k \tag{7}$$

that represent the instantaneous energy and enstrophy fluxes through the k-space bin $|\mathbf{k}| = n\Delta k$. Cascades can be expected when $\gamma \ll 1$ and $T(\mathbf{k})$ is large, such that lossless transport is established over some range of k.

Dynamics.—We simulate the dynamics of neutral point-vortex systems with fixed $L = 10^4 \xi$, fixed dissipation $\gamma = 10^{-4}$ [58,59], and vortex numbers $N = 2^n, n = \{9, 10, \ldots, 15\}$ [60]. The initial conditions are such that only a thin shell of wave numbers of width Δk, localized near an initial wave number k_i, are excited with random

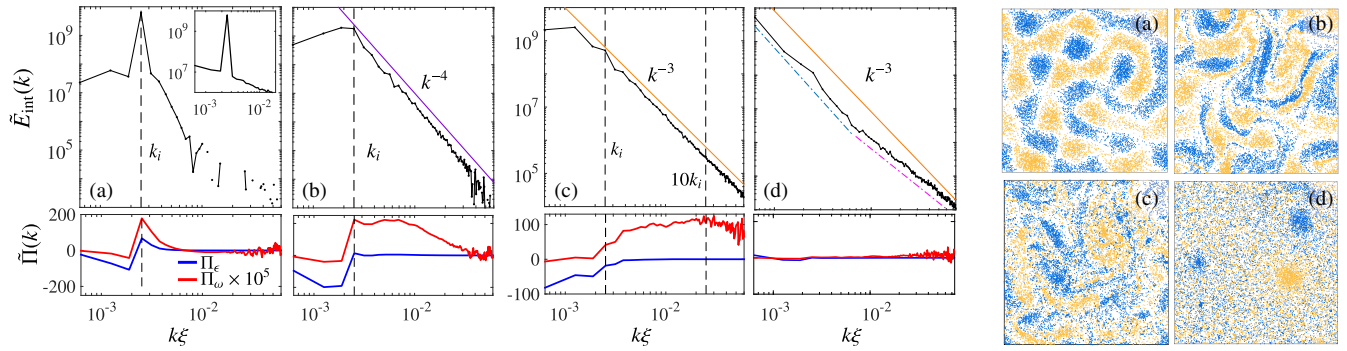

FIG. 1. Kinetic energy spectra and fluxes (in units of $\Gamma^2/4\pi L^2$) and vorticity distributions for $N = 16, 384$ at (a) $t \approx 0.25\tau$, (b) $t \approx 1.85\tau$, and (c) $t \approx 4\tau$ and (d) $t \approx 20\tau$. In (a), at high k, $E_{\rm int}(k)$ is comparatively small and oscillates about zero, causing the broken data line on the log-log scale. Inset shows the full spectrum $E_{\rm self}(k) + E_{\rm int}(k)$ at $t = 0$. Spectra and fluxes are averaged over 4 runs and 9 time samples with time-spacing $\delta t \approx \tau/20$. Note that only the interaction term $E_{\rm int}(k)$ is shown, as the self-energy term only adds a configuration independent N/k scaling. In (d) dash-dot lines are guides to the eye proportional to $k^{-3.2}$ and $k^{-2.2}$.

phases, as is often considered classically [28,52]. To generate such configurations with point vortices, we construct the corresponding classical vorticity field, which is then used as a probability distribution for rejection sampling of quantum vortices [42]. This procedure creates an initial condition with the vast majority of the interaction energy contained within one k mode [Fig. 1(a), inset], even for small vortex numbers $N \sim 10^2$.

The system can be characterized by the superfluid Reynolds number $\mathrm{Re_s}$ [61,62] and the eddy turnover time τ

$$\mathrm{Re_s} = \frac{E_{\rm int}^{1/2} L_i}{\Gamma}, \qquad \tau = \frac{L_i}{\mathrm{v_{rms}}}, \tag{8}$$

where $L_i = 2\pi/k_i$, and $\mathrm{v_{rms}}$ is the root mean square vortex velocity, as per Eq. (2). For a wide range of the localized initial conditions, $E_{\rm int}$ is found to be well approximated by [42]

$$E_{\rm int} = A \times \left(\frac{\Gamma^2}{4\pi L^2}\right)\left(\frac{N}{k_i}\right)^2 (\Delta k)^2, \tag{9}$$

where the constant $A \approx 0.25$. Neglecting unimportant constant factors, this yields a remarkably simple formula for $\mathrm{Re_s}$ as the ratio of two dimensionless quantities,

$$\mathrm{Re_s} = N/n_i^2, \tag{10}$$

where $n_i \equiv k_i/\Delta k$ is the dimensionless initial wave number. To maximize $\mathrm{Re_s}$ while still maintaining approximate isotropy, we thus set $L_i = L/4$. We directly simulate the point-vortex model [Eqs. (1) and (2)] and compute time- and ensemble-averaged spectra and fluxes [Eqs. (4)–(7)], using GPU codes [42,63] that allow us to evaluate the full N-body problem for very large N.

Figures 1(a)–1(c) show examples of the vortex distribution, kinetic energy spectra, and fluxes for $N = 16, 384$ at various times. The qualitative behavior is similar for all N considered, but naturally larger N yields clearer results. Movies of the dynamics for different N are provided in the Supplemental Material [42]. Very early times [Fig. 1(a)] show the spectrum rapidly spreads from the initial state well localized at $k_i = 4(\Delta k)$ [Fig. 1(a), inset]. Shortly after, the spectrum briefly agrees quite well with the Saffman scaling k^{-4}, consistent with the formation of sharp, isolated vorticity-gradient filaments [Fig. 1(b)] [53]. These filaments are repeatedly stretched and packed, and the spectral slope gradually transitions, settling to the k^{-3} scaling from $t \sim 4\tau$ until $t \sim 10\tau$ [Fig. 1(c)]. Thereafter, coherent vortices begin to dominate the distribution, causing the filamentation processes that drives the cascade to become increasingly infrequent. By $t \sim 20\tau$, the vortex distribution is dominated by a few circular coherent vortices [Fig. 1(d)], whose size and number were found to depend on the initial conditions [42]. These structures can be traced back through the dynamics, without interruption, to intensely concentrated clusters in the initial distribution. By this time the k^{-3} spectrum has collapsed; the regions of low and high k in the spectra were found to be very near constant when multiplied by $k^{3.2}$ and $k^{2.2}$, respectively.

Inspection of the energy and enstrophy fluxes confirms the directions of spectral transport. The early developing stages of evolution [Fig. 1(b)] clearly demonstrate the development of a negative energy flux (indicating flow to low k) and positive enstrophy flux (indicating flow to high k) in the mutually exclusive wave number regions $k < k_i$ and $k > k_i$, respectively. The time frame of matured turbulent activity, which exhibits the k^{-3} spectrum, is corroborated by a nearly constant enstrophy flux over approximately one decade of wave numbers [Fig. 1(c)], providing a means to estimate the Kraichnan-Batchelor constant via the compensated kinetic energy spectrum: $C' = E(k)k^3/\eta^{2/3}$, where $\eta = \Pi_\omega$ averaged over k, time window, and ensemble [42]. The late stages dominated by coherent vortices exhibit negligible flux compared to the earlier turbulent dynamics [Fig. 1(d)].

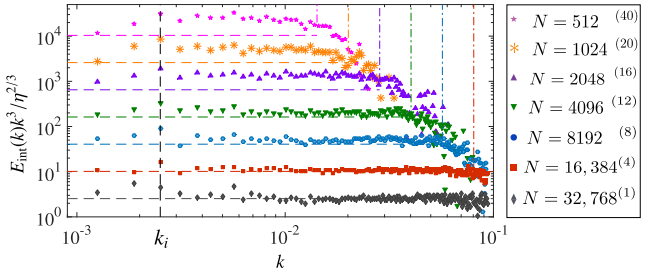

FIG. 2. Compensated kinetic energy spectra for a range of N, averaged over ensemble and a time window $\sim 0.5\tau$. For clarity the spectra are vertically shifted by increasing powers of 4. The horizontal dashed lines shows the value $C' = 1.6$ (also vertically shifted for comparison at different N). Dash-dot lines indicate the intervortex distance wave number k_ℓ at different N (see text). In the legend the bracketed superscripts indicate the number of independent realizations used in the ensemble average.

Figure 2 shows the compensated spectrum for different N at $t \sim 4\tau$. The k^{-3} scaling is observed to some degree for all N considered, albeit over less than a decade for small N ($\sim$0.7 decades for $N = 512$). However, the quality and range of the scaling increases dramatically as N is increased. For smaller N, C' is quite large ($C' \approx 3.8$) [64], but as N increases C' decreases and tends towards a constant value $C' \approx 1.6$. A simulation with $N = 16384$ and $k_f = 8(\Delta k)$ yielded $C' \approx 2.0$, in good agreement with $N = 4096$, $k_f = 4(\Delta k)$, that has the same $\mathrm{Re_s}$ and yielded $C' \approx 1.9$. The scaling range is found to persist up to $k_\ell = 2\pi/\ell$, the wave number associated with the average intervortex distance $\ell = L/N^{1/2}$. Notice that for $N \geq 16\,384$ this means the compensated spectrum is constant over a significant range of roughly 1.5 decades above the initial wave number. Above k_ℓ, the interaction spectrum quickly decreases, indicating a transition from many-vortex to single-vortex physics.

Discussion.—It appears that the basic phenomenology of the decaying enstrophy cascade can indeed be seen in 2DQT: the k^{-3} spectrum readily emerges during the stages of maximum turbulent activity, while the later stages are dominated by coherent vortices that suppress turbulent fluxes. For large $\mathrm{Re_s}$, we also find a Kraichnan-Batchelor constant $C' \approx 1.6$ close to the accepted value for a classical fluid, $C' = 1.4$ [28,65]. Similarly, the Kolmogorov constant in 3D has been found to be the same above and below the λ transition in superfluid He^4 [66]. The observation of greater values of C' at lower $\mathrm{Re_s}$ (although with greater uncertainties) suggests that fewer available degrees of freedom result in less efficient spectral transport in the quantum fluid. Importantly, our results show that $\mathrm{Re_s}$ as defined in Eq. (10) quantifies the degree of turbulence very well, as it can be used to estimate the range of the enstrophy cascade. Since $\mathrm{Re_s} = N(\Delta k/k_i)^2$, our results exhibit the same power-law range scaling as a classical fluid: $k_\ell/k_i \sim \mathrm{Re_s}^{1/2}$. A recent 3DQT experiment [67] also found $\ell^{-1} \sim \mathrm{Re_s}^{3/4}$, similar to the dissipation scale in the Kolmogorov energy cascade. Note, however, here the cascade terminates due to a crossover from many-vortex to single-vortex physics, rather than due to dissipative effects, and suggests that the point-vortex system can effectively be truncated at wave numbers $k \sim k_\ell$, as argued by Kraichnan [68].

Further study is certainly warranted. A more extensive study of the effects of initial conditions is needed to elucidate the role of coherent structures in 2DQT; it seems likely, however, that their influence will be as important as in 2DCT, as here we have already seen, perhaps unsurprisingly, that they readily appear and are dependent on the initial conditions. Furthermore, it now appears probable that the dual inverse-energy and direct-enstrophy cascades [56] could manifest in *forced* 2DQT under the appropriate conditions. Although a previous study showed evidence of the inverse energy cascade in a forced point-vortex model [22], the Kraichnan-Kolmogorov constant was found to be twice the accepted value, seemingly at odds with the results here as well as those from 3DQT. However in Ref. [22] forcing was introduced by essentially reversing the sign of γ. Adapting our rejection-sampling method to *dynamically* introduce vorticity instead could provide a more physical minimal model of forced 2DQT [21]. Studying the forced case would allow a more accurate determination of the Kraichnan-Batchelor constant, but also exploration of intermittency effects [65], and the logarithmic correction in the enstrophy cascade [29,69,70], if large enough vortex numbers and simulations times can be achieved [34,54]. It will also be interesting to explore the relation between the enstrophy cascade observed here and the anomalous scaling at nonthermal fixed points in compressible decaying 2DQT [71,72].

Finally, regarding the prospect of observing the cascade in atomic condensates, the main challenge would be creating a system large enough relative to the healing length ξ, to remain within the low Mach number regime where analogies to the Navier-Stokes equations are valid. For our smallest vortex number, $N = 512$, the Mach number $\mathrm{Ma} = \mathrm{v_{rms}}/c \approx 0.025$ and hence the system size could be reduced to $L/\xi \sim 800$ without invalidating the incompressibility assumption $\mathrm{v_{rms}}/c \lesssim 0.3$ [in Eqs. (1) and (2) $\{\mathbf{x}, L\} \to \lambda\{\mathbf{x}, L\}$ gives $\mathbf{v} \to \lambda^{-1}\mathbf{v}$, $t \to \lambda^2 t$]. For comparison, recent experiments in uniform systems have achieved $L \sim 200\xi$ [7]. While fewer vortices would allow for a smaller system, given the rather limited range of k^{-3} behavior for $N = 512$ it is questionable whether the cascade theory would be valid in systems containing significantly fewer vortices. Nonetheless, full Gross-Pitaevskii simulations for the smaller values of N considered here are well within computational reach, and would provide useful information regarding the effects of physical boundaries, as well as the effects of compressibility and vortex annihilations, which can be tuned through varying the system size for a fixed vortex number and initial condition [38].

Conclusion.—We have numerically observed signatures of an enstrophy cascade in decaying 2DQT, including a k^{-3} power-law spectrum, constant enstrophy flux over a wide inertial range, and a Kraichnan-Batchelor constant converging to $C' \approx 1.6$ for large vortex number. We have shown that the extent of the inertial range scales as $\mathrm{Re}_s^{1/2}$ for a suitably defined superfluid Reynolds number Re_s that depends only on the number of vortices and the length scale where kinetic energy is initially concentrated. The relevance of the classical cascade theory for describing decaying 2DQT suggests some features of decaying turbulence may be universal across classical and quantum fluids. Further insight could be gained by testing measures beyond two-point correlations, such as coherent structure profiles or intermittency statistics. Signatures of the enstrophy cascade become observable for systems of a few hundred vortices, and may soon be within reach of cold-atom 2DQT experiments.

We thank B. P. Anderson for many stimulating discussions and A. J. Groszek for valuable comments. A. S. B. was supported by a Rutherford Discovery Fellowship administered by the Royal Society of New Zealand. M. T. R. was partially supported by the Australian Research Council Centre of Excellence in Future Low-Energy Electronics Technologies (Project No. CE170100039) and funded by the Australian Government.

*m.reeves@uq.edu.au
†thomas.billam@newcastle.ac.uk

[1] L. Onsager, Nuovo Cimento Suppl. **6**, 279 (1949).
[2] W. J. Kwon, G. Moon, J.-y. Choi, S. W. Seo, and Y.-i. Shin, Phys. Rev. A **90**, 063627 (2014).
[3] T. W. Neely, E. C. Samson, A. S. Bradley, M. J. Davis, and B. P. Anderson, Phys. Rev. Lett. **104**, 160401 (2010).
[4] K. E. Wilson, E. C. Samson, Z. L. Newman, T. W. Neely, and B. P. Anderson, Ann. Rev. Cold Atoms Molecules **1**, 261 (2013).
[5] E. C. Samson, K. E. Wilson, Z. L. Newman, and B. P. Anderson, Phys. Rev. A **93**, 023603 (2016).
[6] K. Henderson, C. Ryu, C. MacCormick, and M. G. Boshier, New J. Phys. **11**, 043030 (2009).
[7] G. Gauthier, I. Lenton, N. M. Parry, M. Baker, M. J. Davis, H. Rubinsztein-Dunlop, and T. W. Neely, Optica **3**, 1136 (2016).
[8] S. W. Seo, B. Ko, J. H. Kim, and Y. i. Shin, Sci. Rep. **7**, 4587 (2017).
[9] G. Moon, W. J. Kwon, H. Lee, and Y.-i. Shin, Phys. Rev. A **92**, 051601 (2015).
[10] T. W. Neely, A. S. Bradley, E. C. Samson, S. J. Rooney, E. M. Wright, K. J. H. Law, R. Carretero-González, P. G. Kevrekidis, M. J. Davis, and B. P. Anderson, Phys. Rev. Lett. **111**, 235301 (2013).
[11] A. L. Fetter, Phys. Rev. **151**, 100 (1966).
[12] A. Lucas and P. Surówka, Phys. Rev. A **90**, 053617 (2014).
[13] W. J. Kwon, J. H. Kim, S. W. Seo, and Y. Shin, Phys. Rev. Lett. **117**, 245301 (2016).
[14] T. Frisch, Y. Pomeau, and S. Rica, Phys. Rev. Lett. **69**, 1644 (1992).
[15] A. Finne, T. Araki, R. Blaauwgeers, V. Eltsov, N. Kopnin, M. Krusius, L. Skrbek, M. Tsubota, and G. Volovik, Nature (London) **424**, 1022 (2003).
[16] M. T. Reeves, T. P. Billam, B. P. Anderson, and A. S. Bradley, Phys. Rev. Lett. **114**, 155302 (2015).
[17] G. K. Batchelor, Phys. Fluids **12**, II-233 (1969).
[18] R. Numasato and M. Tsubota, J. Low Temp. Phys. **158**, 415 (2010).
[19] M. T. Reeves, T. P. Billam, B. P. Anderson, and A. S. Bradley, Phys. Rev. Lett. **110**, 104501 (2013).
[20] D. Kobyakov, A. Bezett, E. Lundh, M. Marklund, and V. Bychkov, Phys. Rev. A **89**, 013631 (2014).
[21] A. Skaugen and L. Angheluta, Phys. Rev. E **95**, 052144 (2017).
[22] E. D. Siggia and H. Aref, Phys. Fluids **24**, 171 (1981).
[23] T. P. Billam, M. T. Reeves, B. P. Anderson, and A. S. Bradley, Phys. Rev. Lett. **112**, 145301 (2014).
[24] T. Simula, M. J. Davis, and K. Helmerson, Phys. Rev. Lett. **113**, 165302 (2014).
[25] X. Yu, T. P. Billam, J. Nian, M. T. Reeves, and A. S. Bradley, Phys. Rev. A **94**, 023602 (2016).
[26] H. Salman and D. Maestrini, Phys. Rev. A **94**, 043642 (2016).
[27] S. Fox and P. A. Davidson, J. Fluid Mech. **659**, 351 (2010).
[28] E. Lindborg and A. Vallgren, Phys. Fluids **22**, 091704 (2010).
[29] R. H. Kraichnan, J. Fluid Mech. **47**, 525 (1971).
[30] J. C. McWilliams, AIP Conf. Proc. **106**, 205 (1984).
[31] R. Benzi, G. Paladin, S. Patarnello, P. Santangelo, and A. Vulpiani, J. Phys. A **19**, 3771 (1986).
[32] P. Santangelo, R. Benzi, and B. Legras, Phys. Fluids A **1**, 1027 (1989).
[33] R. Benzi and R. Scardovelli, Europhys. Lett. **29**, 371 (1995).
[34] G. Boffetta and R. E. Ecke, Annu. Rev. Fluid Mech. **44**, 427 (2012).
[35] In the case of an atomic BEC, one has $\xi = \hbar/\sqrt{\mu m}$, $c = \sqrt{\mu/m}$, and $\Gamma = h/m$, where μ is the chemical potential and m is the mass of a constituent particle.
[36] S. J. Rooney, P. B. Blakie, B. P. Anderson, and A. S. Bradley, Phys. Rev. A **84**, 023637 (2011).
[37] P. Blakie, A. Bradley, M. Davis, R. Ballagh, and C. Gardiner, Adv. Phys. **57**, 363 (2008).
[38] T. P. Billam, M. T. Reeves, and A. S. Bradley, Phys. Rev. A **91**, 023615 (2015).
[39] O. Törnkvist and E. Schröder, Phys. Rev. Lett. **78**, 1908 (1997).
[40] J. H. Kim, W. J. Kwon, and Y. Shin, Phys. Rev. A **94**, 033612 (2016).
[41] L. Pismen, *Vortices in Nonlinear Fields*, International Series of Monographs on Physics (Clarendon Press, Oxford, 1999).
[42] See Supplemental Material at http://link.aps.org/supplemental/10.1103/PhysRevLett.119.184502 for movies of the dynamics, further details of the model and numerical simulations, and an analytic estimate of E_{int}. The Supplemental Material contains additional Refs. [43–50].
[43] C. A. Jones and P. H. Roberts, J. Phys. A **15**, 2599 (1982).

[44] C. A. Jones, S. J. Putterman, and P. H. Roberts, J. Phys. A **19**, 2991 (1986).
[45] W. F. Vinen, Phys. Rev. B **64**, 134520 (2001).
[46] W. F. Vinen and J. J. Niemela, J. Low Temp. Phys. **128**, 167 (2002).
[47] N. G. Parker, A. J. Allen, C. F. Barenghi, and N. P. Proukakis, Phys. Rev. A **86**, 013631 (2012).
[48] C. Nore, M. Abid, and M. E. Brachet, Phys. Rev. Lett. **78**, 3896 (1997).
[49] C. Nore, M. Abid, and M. E. Brachet, Phys. Fluids **9**, 2644 (1997).
[50] D. Montgomery and G. Joyce, Phys. Fluids **17**, 1139 (1974).
[51] D. K. Lilly, Phys. Fluids **12**, II-240 (1969).
[52] D. K. Lilly, J. Fluid Mech. **45**, 395 (1971).
[53] M. E. Brachet, M. Meneguzzi, H. Politano, and P. L. Sulem, J. Fluid Mech. **194**, 333 (1988).
[54] A. Vallgren and E. Lindborg, J. Fluid Mech. **671**, 168 (2011).
[55] J. B. Weiss and J. C. McWilliams, Phys. Fluids A **3**, 835 (1991).
[56] R. H. Kraichnan, Phys. Fluids **10**, 1417 (1967).
[57] R. H. Kraichnan and D. Montgomery, Rep. Prog. Phys. **43**, 547 (1980).
[58] A. S. Bradley and B. P. Anderson, Phys. Rev. X **2**, 041001 (2012).
[59] G. W. Stagg, A. J. Allen, N. G. Parker, and C. F. Barenghi, Phys. Rev. A **91**, 013612 (2015).
[60] The point-vortex approximation requires that $u_{\rm rms} \ll c$, so in this sense, for the given parameters, the largest N simulations are not physically reasonable. However, our choice of L is somewhat arbitrary, and the rescaling $\{\mathbf{x}, L\} \to \lambda\{\mathbf{x}, L\}$ (for fixed ξ) yields $v_{\rm rms} \to v_{\rm rms}/\lambda$.
[61] L. Onsager, in *International Conference of Theoretical Physics* (Science Council of Japan, Kyoto and Tokyo, 1953), pp. 877–880.
[62] The superfluid Reynolds number introduced in Ref. [16] may be more appropriate in the presence of a stirring potential.
[63] H. Nguyen, *GPU Gems 3* (Addison-Wesley, New York, 2008).
[64] Some variation of C' with the initial conditions or Reynolds number is expected [28,54,56].
[65] J. Paret, M.-C. Jullien, and P. Tabeling, Phys. Rev. Lett. **83**, 3418 (1999).
[66] C. F. Barenghi, V. S. L'vov, and P.-E. Roche, Proc. Natl. Acad. Sci. U.S.A. **111**, 4683 (2014).
[67] S. Babuin, E. Varga, L. Skrbek, E. Leveque, and P.-E. Roche, Europhys. Lett. **106**, 24006 (2014).
[68] R. H. Kraichnan, J. Fluid Mech. **67**, 155 (1975).
[69] V. Borue, Phys. Rev. Lett. **71**, 3967 (1993).
[70] C. Pasquero and G. Falkovich, Phys. Rev. E **65**, 056305 (2002).
[71] M. Karl and T. Gasenzer, arXiv:1611.01163.
[72] J. Schole, B. Nowak, and T. Gasenzer, Phys. Rev. A **86**, 013624 (2012).